# $(CN_3H_6)_2\cdot(VO_2)_3(PO_4)(HPO_4)$, a Layered Guanidinium Vanadium(V) Phosphate Related to Hexagonal Tungsten Oxide

**Zsolt Bircsak and William T. A. Harrison***

Department of Chemistry, University of Western Australia, Nedlands, WA 6907, Australia

*Received August 13, 1997*

The hydrothermal synthesis, single-crystal structure, and some physical properties of $(CN_3H_6)_2\cdot(VO_2)_3(PO_4)(HPO_4)$, a new guanidinium vanadium(V) phosphate, are reported. This phase is built up from vertex-sharing layers of $VO_6$ octahedra, which adopt the hexagonal tungsten oxide *motif*. These octahedral layers are capped by P−O and P−OH entities resulting in anionic layers of stoichiometry $[(VO)_3(PO_4)(HPO_4)]^{2-}$. Pairs of guanidinium cations are arrayed in the interlayer regions in a manner that suggests interactions may occur between these species. Crystal data consists of the following: $(CN_3H_6)_2\cdot(VO_2)_3(PO_4)(HPO_4)$, monoclinic, $C2/c$ (No. 15), $a = 12.446(3)$ Å, $b = 7.287(2)$ Å, $c = 17.819(5)$ Å, $\beta = 97.23(3)°$, $Z = 4$.

## Introduction

Vanadium phosphates are of substantial current interest. The layered material $VOPO_4\cdot2H_2O$[1] shows a wide range of redox intercalation reactions. $(VO)_2P_2O_7$ shows great promise as a catalyst for the selective oxidation of butane to maleic anhydride.[2] An astonishing variety of novel framework phases arise from the combination of vanadium/phosphate progenitors and small organic molecules.[3] Recently, a family of closely related alkali metal/ammonium vanadium selenites, $M(VO_2)_3(SeO_3)_2$,[4] and alkali metal/ammonium vanadium methylphosphonates, $M(VO_2)_3(PO_3CH_3)_2$,[5] have been described. These materials have a strongly layered character based on infinite sheets of vertex-sharing $VO_6$ octahedra. The three-ring/six-ring connectivity of the $VO_6$ octahedra is equivalent to a single layer of the three-dimensional phase hexagonal tungsten oxide (*hex*-$WO_3$ or HTO).[6] In the layered phases, the apical oxygen atoms of the infinite vanadium−oxygen sheets are capped by Se (as $[SeO_3]^{2-}$) or $P-CH_3$ (as $[PO_3CH_3]^{2-}$) entities, in the selenites and methylphosphonates, respectively. These phases are complemented by a number of molybdenum and tungsten selenites and methylphosphonates based on the same octahedral layering pattern.[7,8] This significant family of related phases may be classified according to the stacking sequence of the octahedral layers, mode of sheet capping, and octahedral distortions.[8b]

In this paper we report the synthesis and characterization of $(CN_3H_6)_2\cdot(VO_2)_3(PO_4)(HPO_4)$, a new guanidinium vanadium hydrogen phosphate. This is the first layered phase based on the HTO *motif* to incorporate organic, as opposed to inorganic, templating cations.

## Experimental Section

**Synthesis.** $(CN_3H_6)_2\cdot(VO_2)_3(PO_4)(HPO_4)$ was prepared from a mixture of 0.875 g of guanidinium carbonate $[(C(NH_2)_3)_2CO_3]$, 2.240 g of 85% $H_3PO_4$, 0.883 g of $V_2O_5$, 1.245 g of $Mg(NO_3)_2$, and 7 mL of deionized water (starting molar ratio of guanidine:V:P ≈ 1:2:4). The metal precursors were mixed in water, acid was added next, and then the organic component. The mixture, enclosed in a 23-mL Parr Teflon-lined hydrothermal bomb filled approximately to the 50% level, was then heated to 120 °C for 2 days. After the mixture was slowly cooled, the solid product, consisting of 1.503 g of green-yellow crystals and powder (yield based on V = 83%) was recovered from the supernatant liquors by filtration. Reactions which omitted the magnesium nitrate did not produce any $(CN_3H_6)_2\cdot(VO_2)_3(PO_4)(HPO_4)$ and led to an unidentified yellow powder. Reactions in which zinc oxide replaced magnesium nitrate in the starting mixture led to a mixed-phase product containing some crystals of $(CN_3H_6)_2\cdot(VO_2)_3(PO_4)(HPO_4)$ and other unidentified phases.

**Physical Characterization.** X-ray powder diffraction data [Siemens D5000 automated diffractometer, Cu Kα radiation, $\lambda = 1.5418$ Å, $T = 25(2)$ °C] were recorded for well-ground yellow powder of $(CN_3H_6)_2\cdot(VO_2)_3(PO_4)(HPO_4)$. Peak-fitting routines established peak positions relative to the Cu K$\alpha_1$ ($\lambda = 1.540\,56$ Å) wavelength. The data were indexed by comparison with a LAZY-PULVERIX[9] simulation of the single-crystal structure of $(CN_3H_6)_2\cdot(VO_2)_3(PO_4)(HPO_4)$, and

---

* E-mail: wtah@chem.uwa.edu.au.

[1] Jacobson, A. J.; Johnson, J. W.; Brody, J. F.; Scanlon, J. C.; Lewandowski, J. T. *Inorg. Chem.* **1985**, *24*, 1782.

[2] Gorbunova, Y. E.; Linde, S. A. *Dokl. Akad. Nauk SSSR* **1979**, *245*, 584.

[3] (a) Soghomonian, V.; Chen, Q.; Haushalter, R. C.; Zubieta, J.; O'Connor, C. J. *Science* (Washington, DC) **1993**, *259*, 1596. (b) Soghomonian, V.; Chen, Q.; Haushalter, R. C.; Zubieta, J. *Angew. Chem., Int. Ed. Engl.* **1993**, *32*, 610. (c) Soghomonian, V.; Chen, Q.; Haushalter, R. C.; Zubieta, J. *Chem. Mater.* **1993**, *5*, 1690. (d) Soghomonian, V.; Haushalter, R. C.; Chen, Q.; Zubieta, J. *Inorg. Chem.* **1994**, *33*, 1700. (e) Khan, M. I.; Meyer, L. M.; Haushalter, R. C.; Schweizer, A. L.; Zubieta, J.; Dye, J. L. *Chem. Mater.* **1996**, *8*, 43. (f) Bonavia, G.; Haushalter, R. C.; O'Connor, C. J.; Zubieta, J. *Inorg. Chem.* **1996**, 35, 5603. (g) Loiseau, T.; Férey, G. *J. Solid State Chem.* **1994**, *111*, 416. (h) Harrison, W. T. A.; Hsu, K.; Jacobson, A. J. *Chem. Mater.* **1995**, *7*, 2004. (i) Bu, X.; Feng, P.; Stucky, G. D. *J. Chem. Soc., Chem. Commun.* **1995**, 1337.

[4] (a) Vaughey, J. T.; Harrison, W. T. A.; Dussack, L. L.; Jacobson, A. J. *Inorg. Chem.* **1994**, *33*, 4370. (b) Harrison, W. T. A.; Dussack, L. L.; Jacobson, A. J. *Acta Crystallogr.* **1995**, *C51*, 2473.

[5] Harrison, W. T. A.; Dussack, L. L.; Jacobson, A. J. *Inorg. Chem.* **1996**, *35*, 1461.

[6] Tournoux, M.; Ganne, M.; Piffard, Y. *J. Solid State Chem.* **1992**, *96*, 141.

[7] (a) Harrison, W. T. A.; Dussack, L. L.; Jacobson, A. J. *Inorg. Chem.* **1994**, *33*, 6043. (b) Harrison, W. T. A.; Dussack, L. L.; Jacobson, A. J. *Inorg. Chem.* **1995**, *34*, 4774.

[8] (a) Harrison, W. T. A.; Dussack, L. L.; Vogt, T.; Jacobson, A. J. *J. Solid State Chem.* **1995**, *120*, 112. (b) Harrison, W. T. A.; Dussack, L. L.; Vaughey, J. T.; Jacobson, A. J. *J. Mater. Chem.* **1996**, *6*, 81.

[9] Yvon, K.; Jeitschko, W.; Parthe, E. *J. Appl. Crystallogr.* **1977**, *10*, 73.

S0020-1669(97)01021-5 CCC: $15.00

**Table 1.** Powder X-ray Data for $(CN_3H_6)_2\cdot(VO_2)_3(PO_4)(HPO_4)$

| $h$ | $k$ | $l$ | $d_{obs}$ (Å) | $d_{calc}$ (Å) | $\Delta d$ | $I_{rel}$ |
|---|---|---|---|---|---|---|
| 0 | 0 | 2 | 8.812 | 8.816 | −0.005 | 100 |
| 1 | 1 | 0 | 6.259 | 6.262 | −0.003 | 9 |
| 2 | 0 | 0 | 6.160 | 6.162 | −0.002 | 12 |
| 1 | 1 | −1 | 6.028 | 6.025 | 0.003 | 24 |
| 1 | 1 | 1 | 5.783 | 5.784 | −0.002 | 2 |
| 1 | 1 | −2 | 5.265 | 5.268 | −0.003 | 13 |
| 2 | 0 | 2 | 4.776 | 4.774 | 0.002 | 15 |
| 0 | 0 | 4 | 4.414 | 4.408 | 0.006 | 28 |
| 1 | 1 | −4 | 3.719 | 3.719 | 0.000 | 1 |
| 0 | 2 | 0 | 3.635 | 3.635 | 0.000 | <1 |
| 3 | 1 | −1 | 3.582 | 3.583 | −0.001 | 1 |
| 1 | 1 | 4 | 3.499 | 3.500 | −0.001 | 1 |
| 3 | 1 | 1 | 3.432 | 3.432 | 0.000 | 6 |
| 2 | 0 | 4 | 3.387 | 3.388 | −0.001 | 2 |
| 0 | 2 | 2 | 3.362 | 3.361 | 0.001 | 4 |
| 3 | 1 | −3 | 3.217 | 3.217 | 0.000 | 7 |
| 1 | 1 | −5 | 3.161 | 3.161 | 0.000 | 1 |
| 2 | 2 | −1 | 3.121 | 3.118 | 0.003 | 15 |
| 0 | 2 | 3 | 3.088 | 3.092 | −0.003 | 8 |
| 0 | 0 | 6 | 2.939 | 2.939 | 0.000 | 13 |
| 2 | 2 | −3 | 2.841 | 2.840 | 0.000 | 8 |
| 4 | 0 | 2 | 2.800 | 2.800 | 0.000 | 6 |
| 1 | 1 | 6 | 2.597 | 2.597 | 0.000 | 8 |
| 1 | 1 | 7 | 2.286 | 2.286 | 0.000 | 7 |
| 0 | 0 | 8 | 2.204 | 2.204 | 0.000 | 7 |
| 1 | 1 | 8 | 2.038 | 2.038 | 0.000 | 6 |
| 0 | 0 | 10 | 1.763 | 1.763 | 0.000 | 5 |

least-squares refinement was carried out with the program ERACEL[10] to result in monoclinic cell parameters of $a = 12.425(6)$ Å, $b = 7.271(4)$ Å, $c = 17.776(5)$ Å, and $\beta = 97.29(3)°$ ($V = 1593$ Å$^3$). Powder data for $(CN_3H_6)_2\cdot(VO_2)_3(PO_4)(HPO_4)$ are listed in Table 1. No impurity lines were visible in the powder pattern.

Thermogravimetric data for the title compound were collected on a Rigaku thermoflex system. The sample was heated at a ramp rate of 20 °C/min under flowing oxygen. Infrared data were collected from 4000 to 400 cm$^{-1}$ using a Matteson FTIR spectrometer (KBr disk method).

**Single-Crystal Structure Determination.** A suitable crystal of $(CN_3H_6)_2\cdot(VO_2)_3(PO_4)(HPO_4)$ (pleochroic yellow/green rhomb, dimensions ~0.1 × 0.1 × 0.1 mm) was selected and glued to a thin glass fiber with cyanoacrylate adhesive and mounted on a Siemens P4 automated diffractometer (graphite monochromated Mo K$\alpha$ radiation, $\lambda = 0.710\,73$ Å). A *C*-centered monoclinic unit cell was established and optimized by the standard procedures of peak-search, centering, indexing, and least-squares routines (26 peaks, $7° < 2\theta < 25°$).

Intensity data were collected at room temperature [25(2) °C] using the $\theta/2\theta$ scan mode for $2° < 2\theta < 60°$. Intensity standards, remeasured every 100 observations, showed only statistical fluctuations over the course of the data collection. Absorption was monitored by $\psi$ scans, but no correction was applied. The raw intensities were reduced to $F$ and $\sigma(F)$ values, the normal corrections for Lorentz and polarization effects were made, and the equivalent data were merged: 3902 measured reflections merged to 2286 unique data [1594 considered observed according to the criterion $I > 3\sigma(I)$] with $R_{Int} = 0.042$.

The systematic absences in the reduced data ($h0l$, $h + l \neq 2n$; $0k0$, $k \neq 2n$) indicated space groups *Cc* or *C*2/*c*, with intensity statistics suggesting the latter. The essential features of the structure of $(CN_3H_6)_2\cdot(VO_2)_3(PO_4)(HPO_4)$ were established by direct methods[11] in the centrosymmetric space group *C*2/*c* (No. 15), which was assumed for the remainder of the crystallographic study. The remainder of the non-hydrogen atoms were located from Fourier difference maps, and a Larson-type secondary extinction correction[12] was optimized to improve the fit of strong, low-angle reflections which showed a systematic $F_{obs} < F_{calc}$ trend. Hydrogen atoms associated with the guanidinium cation were located geometrically by assuming planar sp$^2$ hybridization about each N atom and an N−H bond length of 0.95 Å. Assuming the presence of vanadium(V) and the guanidinium cation, charge balancing requirements necessitated the presence of one additional proton per formula unit. Even though this H atom occupies a general position and is only 50% occupied (vide infra), it was located in a difference map and found to be attached to a P−O vertex. Restraints were required to ensure a stable refinement of this H atom species. Residuals of $R = 3.58\%$ and $R_w = 3.43\%$ [$w_i = 1/\sigma^2(F)$] were obtained for refinements varying positional and anisotropic thermal parameters for all non-hydrogen atoms and an atom-type isotropic thermal factor for the hydrogen atoms. All the least-squares and subsidiary calculations were performed with the Oxford CRYSTALS[13] system. Crystallographic data are summarized in Table 2.

**Table 2.** Crystallographic Parameters for $(CN_3H_6)_2\cdot(VO_2)_3(PO_4)(HPO_4)$

| | |
|---|---|
| empirical formula | $V_3P_2O_{14}C_2N_6H_{13}$ |
| formula weight | 559.93 |
| crystal system | monoclinic |
| $a$ (Å) | 12.446(3) |
| $b$ (Å) | 7.287(2) |
| $c$ (Å) | 17.819(5) |
| $\beta$ (deg) | 97.23(3) |
| $V$ (Å$^3$) | 1603.2(7) |
| $Z$ | 4 |
| space group | *C*2/*c* (No. 15) |
| $T$ (°C) | 25(2) |
| $\lambda$ (Mo K$\alpha$) (Å) | 0.710 73 |
| $\rho_{calc}$ (g/cm$^3$) | 2.32 |
| $\mu$ (cm$^{-1}$) | 20.0 |
| total data | 3902 |
| observed data[a] | 1594 |
| parameters | 128 |
| min, max $\Delta\rho$ (e/Å$^3$) | −0.50, +0.51 |
| $R(F)$[b] | 3.58 |
| $R_w(F)$[c] | 3.43 |

[a] $I > 3\sigma(I)$ after data merging to 2286 reflections. [b] $R = 100 \times \Sigma||F_o| - |F_c||/\Sigma|F_o|$. [c] $R_w = 100 \times [\Sigma w(|F_o| - |F_c|)^2/\Sigma w|F_o|^2]^{1/2}$ with $w_i = 1/\sigma^2(F)$.

**Table 3.** Atomic Coordinates/Thermal Factors for $(CN_3H_6)_2\cdot(VO_2)_3(PO_4)(HPO_4)$

| atom | $x$ | $y$ | $z$ | $U_{eq}$[a] |
|---|---|---|---|---|
| V(1) | 0.23658(5) | 0.07414(8) | 0.73904(3) | 0.0114 |
| V(2) | 0 | −0.1883(1) | 0.75 | 0.0111 |
| P(1) | 0.30952(7) | 0.3674(1) | 0.62008(5) | 0.0100 |
| O(1) | 0.1032(2) | 0.0482(3) | 0.7242(1) | 0.0131 |
| O(2) | 0.2817(2) | −0.1323(3) | 0.7234(1) | 0.0144 |
| O(3) | 0.2563(2) | 0.1904(3) | 0.6437(1) | 0.0126 |
| O(4) | 0.4037(2) | 0.1738(3) | 0.7708(1) | 0.0143 |
| O(5) | 0.2436(2) | 0.0370(3) | 0.8490(1) | 0.0134 |
| O(6) | −0.0682(2) | −0.1349(3) | 0.6475(1) | 0.0122 |
| O(7) | 0.2956(2) | 0.3803(3) | 0.5332(1) | 0.0148 |
| C(1) | 0.4327(3) | 0.2124(6) | 1.0239(2) | 0.0215 |
| N(1) | 0.3596(3) | 0.1374(5) | 1.0614(2) | 0.0325 |
| N(2) | 0.4232(3) | 0.2025(5) | 0.9497(2) | 0.0334 |
| N(3) | 0.5181(3) | 0.2970(5) | 1.0610(2) | 0.0321 |

[a] $U_{eq}$ (Å$^2$) $= {}^1/_3[U_1 + U_2 + U_3]$ where $U_i$ are the principal components of the ellipsoid.

## Results

**Crystal Structure of $(CN_3H_6)_2\cdot(VO_2)_3(PO_4)(HPO_4)$.** Final atomic positional and thermal parameters are listed in Table 3, and selected geometrical data are presented in Table 4. This material adopts a new crystal structure built up from guanidinium cations and layers of vertex-sharing $VO_6$ and $PO_4/HPO_4$

---

(10) Laughlier, J.; Filhol, A. Program ERACEL, distributed by A. Le Bail, University of Le Mans, France.

(11) Sheldrick, G. M. SHELXS86 User Guide, University of Göttingen, Germany, 1986.

(12) Larson, A. C. *Acta Crystallogr.* **1967**, *23*, 664.

(13) Carruthers, J. R.; Watkin, D. J.; Betteridge, P. W. CRYSTALS User Guide, Chemical Crystallography Laboratory, University of Oxford, U.K., 1997.

**Table 4.** Selected Bond Distances (Å) and Angles (deg) for $(CN_3H_6)_2\cdot(VO_2)_3(PO_4)(HPO_4)$

| | | | |
|---|---|---|---|
| V(1)−O(1) | 1.658(2) | V(1)−O(2) | 1.642(3) |
| V(1)−O(2) | 2.261(3) | V(1)−O(3) | 1.942(2) |
| V(1)−O(4) | 2.209(2) | V(1)−O(5) | 1.970(2) |
| V(2)−O(1) × 2 | 2.232(3) | V(2)−O(4) × 2 | 1.642(2) |
| V(2)−O(6) × 2 | 1.954(2) | P(1)−O(3) | 1.533(3) |
| P(1)−O(5) | 1.535(3) | P(1)−O(6) | 1.538(2) |
| P(1)−O(7) | 1.538(2) | C(1)−N(1) | 1.314(5) |
| C(1)−N(2) | 1.314(5) | C(1)−N(3) | 1.329(5) |
| O(1)−V(1)−O(2) | 103.0(1) | O(1)−V(1)−O(2) | 91.1(1) |
| O(2)−V(1)−O(2) | 165.08(5) | O(1)−V(1)−O(3) | 98.3(1) |
| O(2)−V(1)−O(3) | 99.7(1) | O(2)−V(1)−O(3) | 82.8(1) |
| O(1)−V(1)−O(4) | 165.9(1) | O(2)−V(1)−O(4) | 90.8(1) |
| O(2)−V(1)−O(4) | 74.91(9) | O(3)−V(1)−O(4) | 82.1(1) |
| O(1)−V(1)−O(5) | 93.5(1) | O(2)−V(1)−O(5) | 94.0(1) |
| O(2)−V(1)−O(5) | 80.18(9) | O(3)−V(1)−O(5) | 159.4(1) |
| O(4)−V(1)−O(5) | 82.4(1) | O(1)−V(2)−O(1) | 78.9(1) |
| O(1)−V(2)−O(4) | 167.1(1) | O(1)−V(2)−O(4) | 88.3(1) |
| O(1)−V(2)−O(4) | 167.1(1) | O(4)−V(2)−O(4) | 104.5(2) |
| O(1)−V(2)−O(6) | 81.21(9) | O(1)−V(2)−O(6) | 81.09(9) |
| O(4)−V(2)−O(6) | 95.1(1) | O(4)−V(2)−O(6) | 98.9(1) |
| O(6)−V(2)−O(6) | 157.0(2) | O(3)−P(1)−O(5) | 111.0(1) |
| O(3)−P(1)−O(6) | 110.4(1) | O(5)−P(1)−O(6) | 110.4(1) |
| O(3)−P(1)−O(7) | 109.2(1) | O(5)−P(1)−O(7) | 108.2(1) |
| O(6)−P(1)−O(7) | 107.6(1) | V(1)−O(1)−V(2) | 130.2(1) |
| V(1)−O(2)−V(1) | 140.2(1) | V(1)−O(3)−P(1) | 135.5(2) |
| V(1)−O(4)−V(2) | 146.5(1) | V(1)−O(5)−P(1) | 120.0(1) |
| V(2)−O(6)−P(1) | 126.5(1) | N(1)−C(1)−N(2) | 120.5(4) |
| N(1)−C(1)−N(3) | 120.1(4) | N(2)−C(1)−N(3) | 119.4(4) |

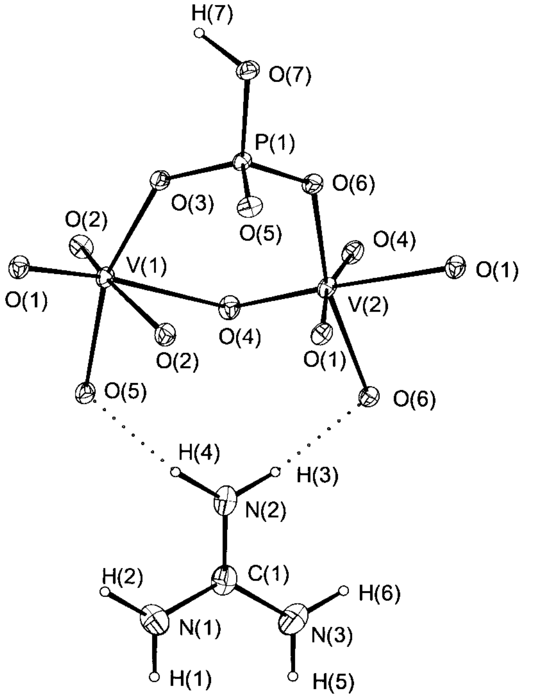

**Figure 1.** CAMERON[23] view of a fragment of the crystal structure of $(CN_3H_6)_2\cdot(VO_2)_3(PO_4)(HPO_4)$ showing the atom-labeling scheme (50% thermal ellipsoids; protons represented by spheres of arbitrary radius, N−H···O hydrogen bonds indicated by dotted lines).

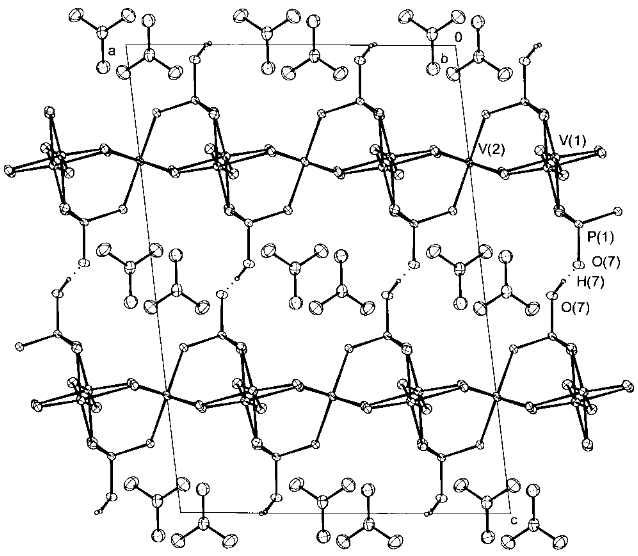

**Figure 2.** View down [010] of the crystal structure of $(CN_3H_6)_2\cdot(VO_2)_3(PO_4)(HPO_4)$ showing the packing of the guanidinium cations (N−H atoms omitted for clarity) into the interlayer regions of the structure. An "eight-ring" channel is formed by the $VO_6$ and $(H)PO_4$ polyhedra in this direction. The 50% occupied H(7) atom is shown occupying only $^1/_2$ its possible sites to emphasize the disordered interlayer H bonding scheme.

units, fused together via V−O−V′ and V−O−P bonds. A fragment of the structure showing the atom-labeling scheme is shown in Figure 1, and the complete crystal structure is illustrated in Figure 2.

There are 14 independent non-hydrogen atoms in $(CN_3H_6)_2\cdot(VO_2)_3(PO_4)(HPO_4)$, all of which occupy general positions, except V(2), which has 2-fold symmetry. The two distinct vanadium atoms are both octahedrally coordinated by oxygen atom neighbors. Both of these $VO_6$ octahedra show a distinctive octahedral distortion mode, in which the vanadium atom has made a nominal shift from the centroid of its octahedron toward an octahedral edge (a so-called local [110] distortion[4]). This results in two short ($d$ < 1.66 Å) V−O bonds in cis configuration, each of which is trans to a long ($d$ > 2.20 Å) V−O link. The remaining two V−O bonds are of intermediate length. Analysis of the $VO_6$ octahedra with the program IVTON[14] showed that V(1) and V(2) were displaced from the centroids of their coordination polyhedra by 0.41 Å and 0.42 Å, respectively. Octahedral volumes of 9.51 $Å^3$ and 9.46 $Å^3$ resulted for the $V(1)O_6$ and $V(2)O_6$ groups, respectively. Bond valence sum (BVS) calculations[14] yielded values of 4.98 for V(1) and 5.05 for V(2) [expected value = 5.00 for vanadium(V) character]. The individual bond valences of the short V−O bonds are >1.5, more than twice as large as those of the longer V−O links. The $PO_4/HPO_4$ group is a typical tetrahedron with $d_{av}(P-O) = 1.536$ Å and BVS(P) = 4.98; three P−O−V bonds and one terminal P−O/P−OH linkage are formed by this group. This 50% occupied H(7) atom, as modeled here, is displaced from an inversion center [apparent $d(H\cdots H) \approx 0.7$ Å]. It is attached to O(7) and hydrogen bonds to a similar O atom ($d[O(7)\cdots O(7)] = 2.44$ Å) in an adjacent layer [via O(7)−H(7)···O(7)′ or O(7)···H(7)−O(7)′ links, see Figure 2]. Although the scattering contribution of H(7) is marginally above the noise level in the data, support for its location in the intersheet region is provided by the bond valence of O(7), which is only 1.2 when considering its connectivity to P. The position of H(7) is chemically reasonable, but its presence could only be unambiguously demonstrated through the use of neutron diffraction data. The layer stoichiometry is $[(VO_2)_3(PO_4)(HPO_4)]^{2-}$, with charge compensation provided by a crystallographically equivalent pair of protonated guanidinium cations occupying the interlayer region. The guanidinium cation shows typical, equivalent C−N bond lengths [average = 1.319 Å], as seen in other framework compounds templated by this cation.[15]

---

(14) Zunic, T. B.; Vickovic, I. *J. Appl. Crystallogr.* **1996**, *29*, 305.
(15) Harrison, W. T. A.; Phillips, M. L. F. *Chem. Mater.* **1997**, *9*, 1837.

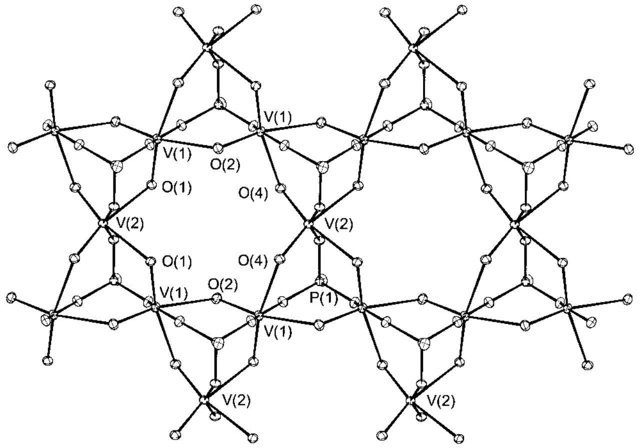

**Figure 3.** View down [001] of part of a $(VO_2)_3(PO_4)(HPO_4)$ layer in $(CN_3H_6)_2\cdot(VO_2)_3(PO_4)(HPO_4)$ showing the arrangement of capped three rings and six rings of $VO_6$ octahedra. Note that in a particular sheet, all the V(2) species are displaced from the centers of their octahedra in the same direction. This displacement occurs in the opposite sense in adjacent sheets.

The structural motif in $(CN_3H_6)_2\cdot(VO_2)_3(PO_4)(HPO_4)$ consists of infinite sheets of vertex-sharing $VO_6$ octahedra, which are linked into triangles (three-rings) of two V(1)- and one V(2)-centered units and six-ring windows (Figure 3). Thus, each $VO_6$ octahedron makes four in-sheet (axial) linkages to adjacent octahedra, with these axial bonds approximately aligned in the *ab* plane. Every V−O−V bridge involves a short V═O and a long V−O bond. Three adjacent apical V−O bonds in each three-ring are capped by a P−O(H) entity, thus forming a tetrahedral (hydrogen) phosphate group. These $PO_4$/$HPO_4$ groups occur on both faces of the vanadium/oxygen sheet. The arrangement of the P−O entities is strictly ordered. In the crystal structure model used here, the attachment of the 50% occupied H(7) atoms to the terminal P−O bonds is completely random (Figure 2). An ordered array of $PO_4$ and $HPO_4$ groups requires symmetry lowering to space group *Cc*. Attempted refinements in this space group were unsuccessful and led to high correlations and higher residuals.

The anionic layers in this material stack normal to the *ab* plane, with an *ABAB*... repeat pattern. The interlayer separation is approximately 8.84 Å, as measured from V-atom−plane to V-atom−plane. Polyhedral eight-ring channels formed from $VO_6$ and (H)$PO_4$ units (incorporating H-bonding linkages) are apparent when the structure is viewed down the [010] and $[\bar{1}10]$ directions. The offset stacking arrangement of the layers means that there are no [001] channels equivalent to the [001] six-ring channels seen in hexagonal $WO_3$.[6]

The guanidinium cations occupy the interlayer regions (Figure 4). On the basis of the geometrical placement of the hydrogen atoms described above, the H-bonding pattern of this species involves four stronger N−H···O bonds with $d$(H···O) < 2.10 Å and two much weaker bonds with 2.30 Å < $d$(H···O) < 2.32 Å. These H bonds involve linakges to terminal P−O/P−OH and bridging V−O−P oxygen atom acceptors. The two longer H bonds are barely significant on the basis of bond valence calculations ($V$ < 0.06 for each bond). Interestingly, the guanidinium species does not form any *interlayer* H bonds: when considering the four shorter N−H···O interactions, all four of these H bonds are to one sheet. Within a particular eight-ring channel, the guanidinium cations appear to stack in such a way that the planes of pairs of molecules are roughly parallel and separated by ~3.5 Å, which is reminiscent of the characteristic stacking separation of this cation in some molecular crystals.[16] Molecular dynamic studies[17] of the guanidinium cation in aqueous solution suggest that an energy minimum occurs when stacked pairs of $[CN_3H_6]^+$ cations are separated by ~3.3 Å, i.e., electrostatic cation−cation repulsion is presumably overcome by favorable solvation effects. Thus, it is possible that an intimate solvated ion pair of two guanidinium cations is acting as a large templating species in the formation of $(CN_3H_6)_2\cdot(VO_2)_3(PO_4)(HPO_4)$.

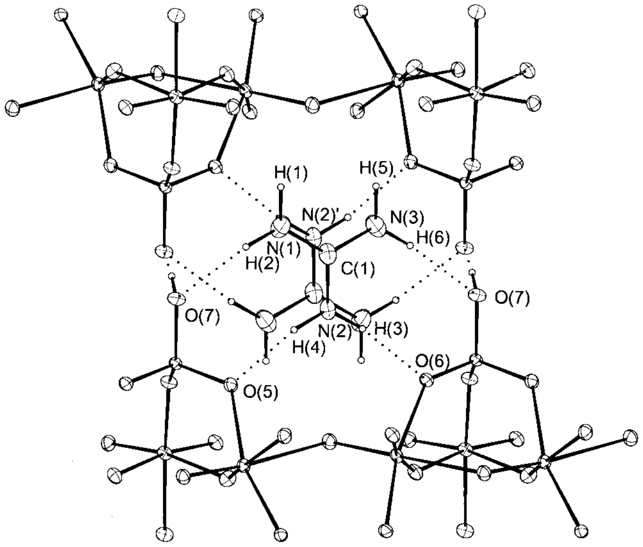

**Figure 4.** Detail of the $(CN_3H_6)_2\cdot(VO_2)_3(PO_4)(HPO_4)$ structure showing the H bonding of the guanidinium cations. Note that one molecule only makes H bonding links to one adjacent sheet when interactions shorter that 2.2 Å are considered. The intermolecular distance C(1)···N(2)′ is 3.51 Å.

**Physical Data.** TGA for $(CN_3H_6)_2\cdot(VO_2)_3(PO_4)(HPO_4)$ showed a two-step weight loss of 27.7% from 300 °C to 500 °C and then a weight increase of 1.2% from 500 °C to 650 °C. The initial weight loss can be attributed to the exothermic loss of the templating agent $(C(NH_2)_3)^+$ (calculated loss 26.2%, observed loss 25.2%). The phenomenon of weight loss followed by weight gain may be attributed to partial reduction of V during template decomposition, followed by reoxidation.

The infrared spectrum of $(CN_3H_6)_2\cdot(VO_2)_3(PO_4)(HPO_4)$ is shown in Figure 5. Prominent bands attributable to C−N, N−H, P−O, and V−O vibrational modes may be assigned by comparison with IR data for related structures.[4] Bands in the 3200−3450 $cm^{-1}$ region can be attributed to N−H stretching, while those in the 1650 to 1700 $cm^{-1}$ region and at 850 and 930 $cm^{-1}$ are due to H−N−H bending modes. C−N stretching bands can be observed in the 1400 to 1600 $cm^{-1}$ region. The peak at 815 $cm^{-1}$ may be due to a V═O stretch or a V−O−V mode. The peak at 1010 $cm^{-1}$ is due to a P−O stretch.

## Discussion

A new guanidinum vanadium(V) hydrogen phosphate, $(CN_3H_6)_2\cdot(VO_2)_3(PO_4)(HPO_4)$, has been prepared by hydrothermal methods and has been structurally and physically characterized. Pure vanadium(V) character is well-defined in this phase on the basis of BVS calculations, geometry, charge balancing, and crystal color. As is typical of kinetically controlled, solvent-mediated reactions,[18] there is no particular correlation between the reaction starting composition and the

---

(16) (a) Cotton, F. A.; Day, V. W.; Hazen, E. E.; Larsen, S. *J. Am. Chem. Soc.* **1973**, *95*, 4834. (b) Harrowfield, J. M. *J. Chem. Soc., Dalton Trans.* **1996**, 3165.

(17) Boudon, S.; Wipff, G.; Maigret, B. *J. Phys. Chem.* **1990**, *94*, 6056.

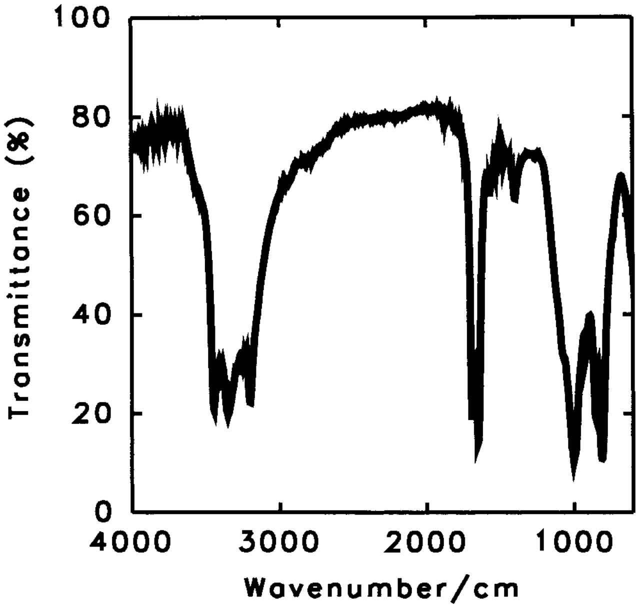

**Figure 5.** IR spectrum of $(CN_3H_6)_2\cdot(VO_2)_3(PO_4)(HPO_4)$.

majority solid-phase product stoichiometry, although by careful empirical adjustment of the reaction conditions, a good yield was obtained. However, without the addition of the metal cations $Mg^{2+}$ or $Zn^{2+}$, $(CN_3H_6)_2\cdot(VO_2)_3(PO_4)(HPO_4)$ does not form at all under any other synthesis conditions tried thus far. At present, the role of these metallic cations is unknown but not unprecedented; for example, a barium vanadium(IV) phosphate hydrate, $Ba_2VO(PO_4)_2\cdot H_2O$,[19] required the presence of $Zn^{2+}$ to form, although no zinc was incorporated in the majority product.

Structurally, $(CN_3H_6)_2\cdot(VO_2)_3(PO_4)(HPO_4)$ has a strongly layered character. The octahedral linkage pattern is identical to that found in the HTO-type $M(VO_2)_3(SeO_3)_2$[4] and $M(VO_2)_3(PO_3CH_3)_2$[5] phases noted in the Introduction. $(CN_3H_6)_2\cdot(VO_2)_3(PO_4)(HPO_4)$ is related to these phases but also shows some significant new features. It is the first HTO-type layered phase to show offset *ABAB*... layers, compared to all the other phases in this family[8b] where the stacking pattern of anionic sheets (in an *ABAB*... or *ABCABC*... pattern) results in either a 3-fold or a 6-fold symmetry axis normal to the layers.

$(CN_3H_6)_2\cdot(VO_2)_3(PO_4)(HPO_4)$ is the first layered vanadium HTO compound containing hydrogen phosphate as the capping group. The layered phase $SrAl_3(OH)_6(PO_4)(HPO_4)$, containing both phosphate and hydrogen phosphate groups has been previously reported,[20] but the stacking motif and interlayer species is quite different in this material to the situation observed for $(CN_3H_6)_2\cdot(VO_2)_3(PO_4)(HPO_4)$. The octahedral Al atom occupies an inversion center in $SrAl_3(OH)_6(PO_4)(HPO_4)$, compared to the highly distorted $VO_6$ octahedra found in $(CN_3H_6)_2\cdot(VO_2)_3(PO_4)(HPO_4)$.

The vanadium-to-vanadium interlayer separation in $(CN_3H_6)_2\cdot(VO_2)_3(PO_4)(HPO_4)$ of 8.84 Å is much larger than those observed in the related alkali metal/ammonium vanadium selenites and methylphosphonates, where an interlayer separation of 5.7−6.4 Å is found, depending on the interlayer cation type. Doubtless this is partially due to the increased steric requirements of the guanidinium cation. Interestingly, however, $(CN_3H_6)_2\cdot(VO_2)_3(PO_4)(HPO_4)$ is the only phase in this family to show interlayer H bonding from capping group to capping group, which is geometrically possible because of the offset layers.

The distinctive and unusual local [110] $VO_6$ distortion mode that occurs in $(CN_3H_6)_2\cdot(VO_2)_3(PO_4)(HPO_4)$ also occurs in the $M(VO_2)_3(SeO_3)_2$ and $M(VO_2)_3(PO_3CH_3)_2$ phases. Such distortions of octahedral $d^0$ species may be theoretically understood in terms of a second-order Jahn−Teller effect. However, it is difficult to predict the direction and magnitude of such distortions from first principles.[21] Most other octahedral vanadium(V)-containing phases show a local [100] distortion, in which the V atom is displaced toward a single O atom neighbor, resulting in a single short V═O (or "vanadyl") bond trans to a long V−O link and in four intermediate-length V−O bonds.[22] For the $M(VO_2)_3(PO_3CH_3)_2$ methylphosphonates, it was suggested that the local [110] distortion might arise in order to maximize cation−cation separation for the vanadium species. Applying a similar argument to $(CN_3H_6)_2\cdot(VO_2)_3(PO_4)(HPO_4)$ results in an average V···V distance of 3.634 Å in a particular octahedral three-ring, compared to 3.619 Å for model structure with V atoms located at their octahedral centroids. We are continuing our investigations into vanadium/phosphate phases templated by small organic entities.

**Acknowledgment.** We thank the Australian Research Council for financial support.

**Supporting Information Available:** Tables of hydrogen atom positions and anisotropic thermal factors (1 page). Ordering information is given on any current masthead page.

IC9710216

---

(18) Harrison, W. T. A.; Dussack, L. L.; Jacobson, A. J. *J. Solid State Chem.* **1996**, *125*, 234.

(19) Harrison, W. T. A.; Lim, S. C.; Vaughey, J. T., Jacobson, A. J.; Goshorn, D. P.; Johnson, J. W. *J. Solid State Chem.* **1994**, *113*, 444.

(20) Kato, T. *Mineral. J.* **1987**, *13*, 390.

(21) Kunz, M.; Brown, I. D. *J. Solid State Chem.* **1995**, *115*, 395.

(22) Jordan, B.; Calvo, C. *Can. J. Chem.* **1973**, *51*, 2621.

(23) Pearce, L. M.; Prout, C. K.; Watkin. D. J. CAMERON user guide, Chemical Crystallography Laboratory, University of Oxford, U.K., 1995.